Inorg. Chem. **2006**, *45*, 5429–5437

Syntheses and Characterization of Oxygen/Sulfur-Bridged Incomplete Cubane-Type Clusters, $[Mo_3S_4Tp_3]^+$ and $[Mo_3OS_3Tp_3]^+$, and a Mixed-Metal Cubane-Type Cluster, $[Mo_3FeS_4ClTp_3]$. X-ray Structures of $[Mo_3S_4Tp_3]Cl$, $[Mo_3OS_3Tp_3]PF_6$, and $[Mo_3FeS_4ClTp_3]$

Tsutomu Yamauchi,[†] Hideaki Takagi,[‡] Takashi Shibahara,[§] and Haruo Akashi*[,†]

Research Institute of Natural Sciences, Okayama University of Science, Ridai-cho, Okayama 700-0005, Japan, Department of International Conservation Studies for Cultural properties, KIBI International University, Takahashi-shi, Okayama 716-0018, Japan, and Department of Chemistry, Okayama University of Science, Ridai-cho, Okayama 700-0005, Japan

Received February 20, 2006

The reaction of $[Mo_3S_4(H_2O)_9]^{4+}$ (**1**) with hydrotris(pyrazolyl)borate (Tp) ligands produced $[Mo_3S_4Tp_3]Cl\cdot 4H_2O$ ([**3**]-$Cl\cdot 4H_2O$) in an excellent yield. An X-ray structure analysis of [**3**]$Cl\cdot 4H_2O$ revealed that each molybdenum atom bonded to the Tp ligand. We report four salts of **3**, [**3**]$Cl\cdot 4H_2O$, [**3**]$tof\cdot 2H_2O$, [**3**]$PF_6\cdot H_2O$, and [**3**]$BF_4\cdot 2H_2O$ in this paper. The solubility and stability of the chloride salt in organic solvents differ completely from those of the other salts. We have also prepared a new compound, $[Mo_3OS_3Tp_3]PF_6\cdot H_2O$ ([**4**]$PF_6\cdot H_2O$), via the reaction of $[Mo_3OS_3(H_2O)_9]^{4+}$ (**2**) with KTp in the presence of NH_4PF_6. All the molybdenum atoms bonded to Tp ligand. ^{1}H NMR signals corresponding to nine protons bonded to three pyrazole rings in one Tp were observed in a spectrum (at 253 K) of [**3**]$BF_4\cdot 2H_2O$. It shows that cluster **3** has a 3-fold rotation axis in CD_2Cl_2 solution. Twenty-one ^{1}H NMR signals corresponding to twenty-seven protons bonded to nine pyrazole rings in three Tp ligands were observed in a spectrum (at 233 K) of [**4**]$PF_6\cdot H_2O$; obviously, **4** has no 3-fold rotation axis, in contrast to **3**. The short CH$\cdots\mu_3$S distance caused large upfield chemical shifts in the ^{1}H NMR spectra of **3** and **4**. The reaction of **3** with metallic iron in CH_2Cl_2 produced $[Mo_3FeS_4XTp_3]$ (X = Cl (**5**), Br (**6**)). X-ray structure analysis of **5** has revealed the existence of a cubane-type core Mo_3FeS_4. Complex **3** functions as a metal-complex ligand for preparing a novel mixed-metal complex even in nonaqueous solvents. The cyclic voltammogram of **5** shows two reversible one-electron couples ($E_{1/2}$ = –1.40 and 0.52 V vs SCE) and two irreversible one-electron oxidation processes (E_{pc} = 1.54 and 1.66 V vs SCE).

Introduction

Over the past decade, syntheses of a series of mixed-metal cubane-type clusters containing Mo_3MS_4 (M = metals) cores have been created via a reaction of $[Mo_3S_4(H_2O)_9]^{4+}$ (**1**)[1] with metals,[2,3] metal ions,[2e,2j] and organometallic compounds.[4] Recently, the chemistry of mixed-metal Mo_3MS_4 clusters has been extended to nonaqueous solution.[5] Although the catalytic activity of the complexes has been expected, only a few examples of such catalytic functions of the

* To whom correspondence should be addressed. E-mail: akashi@high.ous.ac.jp.
† Research Institute of Natural Sciences, Okayama University of Science.
‡ KIBI International University.
§ Department of Chemistry, Okayama University of Science.

(1) (a) Sakane, G.; Shibahara, T. *Inorg. Synth.* **2002**, *33*, 144. (b) Shibahara, T.; Akashi, H. *Inorg. Synth.* **1992**, *29*, 260. (c) Shibahara, T. *Adv. Inorg. Chem.* **1991**, *37*, 143. (d) Akashi, H.; Shibahara, T.; Kuroya, H. *Polyhedron* **1990**, *9*, 1671.

(2) Fe: (a) Shibahara, T.; Akashi, H.; Kuroya, H. *J. Am. Chem. Soc.* **1986**, *108*, 1342. (b) Shibahara, T.; Sakane, G.; Naruse, Y.; Taya, K.; Akashi, H.; Ichimura, A.; Adachi, H. *Bull. Chem. Soc. Jpn.* **1995**, *68*, 2769. Co and Hg: (c) Shibahara, T.; Akashi, H.; Yamasaki, M.; Hashimoto, K. *Chem. Lett.* **1991**, 689. Ni: (d) Shibahara, T.; Sakane, G.; Naruse, Y.; Taya, K.; Akashi, H.; Ichimura, A.; Adachi, H. *Bull. Chem. Soc. Jpn.* **1995**, *68*, 2769. Cu: (e) Shibahara, T.; Akashi, H. *Inorg. Chim. Acta* **2000**, *300/302*, 572. Ga: (f) Shibahara, T.; Kobayashi, S.; Tuji, N.; Sakane, G.; Fukuhara, M. *Inorg. Chem.* **1997**, *36*, 1702. In: (g) Sakane, G.; Shibahara, T. *Inorg. Chem.* **1993**, *32*, 777. (h) Sakane, G.; Yao, Y.; Shibahara, T. *Inorg. Chim. Acta* **1994**, 13, 216. Pd: (i) Murata, T.; Gao, H.; Mizobe, Y.; Nakano, F.; Motomura, S.; Tanase, T.; Yano, S.; Hidai, M. *J. Am. Chem. Soc.* **1992**, *114*, 8287. Sn: (j) Akashi, H.; Shibahara, T. *Inorg. Chem.* **1989**, 28, 2906. Sb: (k) Sakane, G.; Hashimoto, K.; Takahashi, M.; Takeda, M.; Shibahara, T. *Inorg. Chem.* **1998**, 37, 4231. (l) Shibahara, T.; Hashimoto, K.; Sakane, G. *J. Inorg. Biochem.* **1991**, 43.

10.1021/ic060293i CCC: $33.50
Published on Web 06/07/2006

Scheme 1

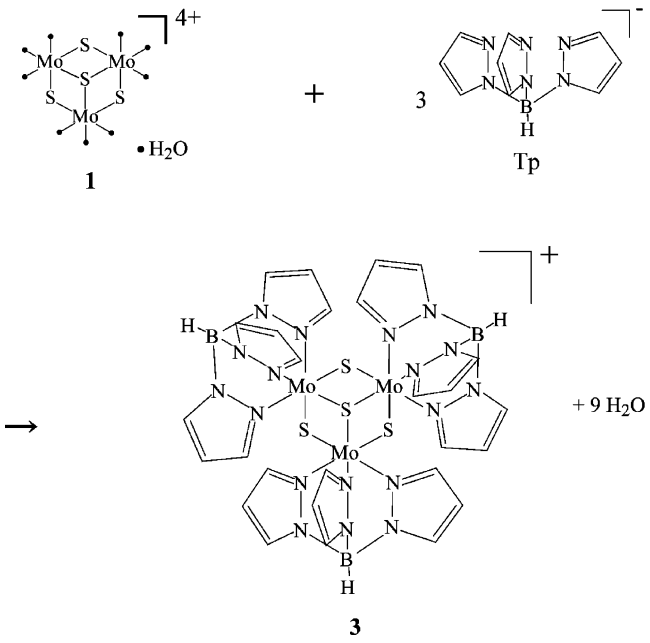

complexes with Mo_3MS_4 cores have been reported.[6] We have prepared clusters with hindered hydrotris(pyrazolyl)borate (Tp) ligands, $[Mo_3S_4Tp_3]^+$ (**3**) and $[Mo_3OS_3Tp_3]^+$ (**4**). Since Tp, which is highly soluble in common organic solvents, has been used as a molecular vise to keep the molybdenum ion in a firm tridentate grip, undesired chemical reactions could be prevented at the molybdenum coordination sites (Scheme 1).

Although the complexes have been described for most elements of group 1 through 13,[7] $[\{Mo_3S_4Tp_2\}_2(\mu\text{-O})(\mu\text{-pz})_2]\cdot 2THF$ ([**7**]·2THF)[8] is the only example so far of a Tp cluster containing a Mo_3S_4 core. In this paper, an X-ray structure analysis of $[Mo_3S_4Tp_3]Cl\cdot 4H_2O$ ([**3**]Cl·$4H_2O$) revealed that each molybdenum atom bonded to the ligand Tp. We also successfully isolated $[Mo_3FeS_4ClTp_3]$ (**5**) and $[Mo_3FeS_4BrTp_3]$ (**6**) clusters from the reaction of **3** with metallic iron.

Experimental Section

Materials. Tetrabutylammonium hexafluoroposphate ($TBAPF_6$, Fluka, electrochemical grade,) and dichloromethane anhydrous (Aldrich) were used as received.

Syntheses of Oxygen/Sulfur-Bridged Incomplete Cubane-Type Clusters with Tp Ligands. [3]Cl·$4H_2O$ (fw 1180.69). A green solution of cluster **1** (in 2 M HCl, 0.17 M per trimer, 5.0 mL, 0.86 mmol) was evaporated to dryness in a vacuum. The green residue was dissolved in methanol (10 mL) to generate a green solution. A methanol solution (10 mL) containing $K(C_9H_{10}N_6B)$ (KTp, 647.0 mg, 2.6 mmol) was added to the green solution and stirred overnight. Green microcrystals of [**3**]Cl·$4H_2O$ and KCl powder precipitated together during stirring. The precipitates were collected by filtration and washed with water to remove the KCl powder. Green microcrystals of [**3**]Cl·$4H_2O$ were obtained in about an 86% yield (867 mg). Anal. Calcd for $C_{27}H_{38}B_3ClMo_3N_{18}O_4S_4$: C, 27.89; H, 3.29; N, 21.68. Found: C, 27.74; H, 2.53; N, 21.45. ^{1}H NMR (CD_3OD, 20 °C): δ 5.92 (s, 1H), 5.97 (s, 1H),6.44 (d, 1H), 6.79 (t, 1H), 7.99 (s, 1H), 8.23 (s, 1H), 8.42 (s, 1H), 8.48 (d, 1H), 8.54 (d, 1H)).

[3]tof·$2H_2O$ (fw 1240.26). Sodium trifluoromethanesulfonate $NaCF_3SO_3$ (Natof, 328 mg, 1.9 mmol) was added to a methanol solution containing [**3**]Cl·$4H_2O$ (450 mg, 0.38 mmol). The mixture was stirred overnight. Green crystals of [**3**]tof·$2H_2O$ were deposited during stirring. Yield: 380 mg, 80%. Anal. Calcd for $C_{28}H_{34}B_3F_3Mo_3N_{18}O_5S_5$: C, 27.12; H, 2.76; N, 20.28. Found: C, 27.25; H, 2.23; N, 20.33. ^{1}H NMR(CD_2Cl_2, 20 °C): δ 5.82 (d, 1H), 5.83 (s, 1H), 6.24 (t, 1H), 6.65 (t, 1H), 7.75 (d, 1H), 8.10 (d, 1H), 8.13 (d, 1H), 8.24 (d, 1H), 8.36 (d, 1H)).

[3]PF_6·H_2O (fw 1218.14). $TBAPF_6$ (738 mg, 1.9 mmol) was added to a methanol solution containing [**3**]Cl·$4H_2O$ (450 mg, 0.38 mmol). The mixture was stirred overnight. Green crystals of [**3**]-PF_6·H_2O were deposited during stirring. Yield: 397 mg, 82%. Anal. Calcd for $C_{27}H_{32}B_3F_6Mo_3N_{18}OPS_4$: C, 26.62; H, 2.65; N, 20.70. Found: C, 26.79; H, 2.08; N, 20.60. ^{1}H NMR (CD_2Cl_2, 20 °C): δ 5.82 (d, 1H), 5.83 (s, 1H), 6.26 (t, 1H), 6.65 (t, 1H), 7.74 (d, 1H), 8.11 (d, 1H), 8.12 (d, 1H), 8.24 (d, 1H), 8.35 (d, 1H)).

[3]BF_4·$2H_2O$ (fw 1178.0). Tetrabutylammonium tetrafluoroborate ($TBABF_4$, 628 mg, 1.9 mmol) was added to a methanol solution containing [**3**]Cl·$4H_2O$ (450 mg, 0.38 mmol). The mixture was stirred overnight. Green crystals of [**3**]BF_4·$2H_2O$ were deposited during stirring. Yield: 324 mg, 72%. Anal. Calcd for $C_{27}H_{34}N_{18}B_4F_4Mo_3O_2S_4$: C, 27.53; H, 2.91; N, 21.41. Found: C, 27.86; H, 2.25; N, 21.39. ^{1}H NMR (CD_2Cl_2, 20 °C): δ 5.82 (d, 1H), 5.83 (s, 1H),6.26 (t, 1H), 6.65 (t, 1H), 7.75 (d, 1H), 8.10 (d, 1H), 8.12 (d, 1H), 8.24 (d, 1H), 8.35 (d, 1H)), (CD_2Cl_2, −20 °C): δ = 5.80 (t, 1H), 5.82 (d, 1H),6.25 (t, 1H), 6.64 (t, 1H), 7.74 (d, 1H), 8.09 (d, 1H), 8.11 (d, 1H), 8.23 (d, 1H), 8.33 (d, 1H)).

[4]PF_6·H_2O (fw 1202.07). A green solution of cluster **2** (in 2 M HCl, 0.17 M per trimer, 1.0 mL, 0.17 mmol) was evaporated to dryness in a vacuum. The green residue was dissolved in methanol (1 mL) to generate a green solution. NH_4PF_6 (108.4 mg, 0.67 mmol) was added to the solution, followed by the addition of a methanol solution (1 mL) containing KTp (108.4 mg, 0.67 mmol). The mixture was stirred overnight. Green microcrystals of [**4**]PF_6·H_2O and white powder precipitated together during stirring. The white powder may be a mixture of KCl and NH_4Cl. The precipitates were collected by filtration and washed with water to remove the white powder. Green microcrystals of [**4**]PF_6·H_2O were obtained in about

(3) Sakane, G.; Shibahara, T. *Inorg. Synth.* **2002**, *33*, 150.
(4) Rh: (a) Akashi, H.; Isobe, K.; Shibahara, T. *Inorg. Chem.* **2005**, *44*, 3494. Pt, Rh, Re: (b) Sokulov, N. M.; Villagra, D.; El-Hendawy, M. A.; Kwak, C.; Elsegood, M. R. J.; Clegg, W.; Sykes, G. *J. Chem. Soc., Dalton Trans.* **2001**, 2611.
(5) Zn: (a)Sakane, G.; Kawasaki, H.; Oomori, T.; Yamasaki, M.; Adachi, H.; Shibahara, T. *J. Cluster Sci.* **2002**, *13*, 75. Cd: (b) Sakane, G.; Kawasaki, H.; Yamasaki, M.; Adachi, H.; Shibahara, T. *Chem. Lett.* **1999**, 631. Ru, Ni, and Pd: (c) Takei, I.; Suzuki, K.; Enta, Y.; Dohki, K.; Suzuki, T.; Mizobe, Y.; Hidai, M. *Organometallics* **2003**, *22*, 1790. Ni, Pd, and Pt: (d) Herbst, K.; Zanello, P.; Corsini, M.; D'Amelio, N.; Dahlenburg, L.; Brorson, M. *Inorg. Chem.* **2003**, *42*, 974. Ru, Os, Rh, and Ir: (e) Herbst, K.; Monari, M.; Brorson, M. *Inorg. Chem.* **2001**, *40*, 2979. Pt: (f) Masui, D.; Ishii, Y.; Hidai, M. *Bull. Chem. Soc. Jpn.* **2000**, *73*, 931. Pt: (g) Saito, T.; Tsuboi, T.; Kajitani, Y.; Yamagata, T.; Imoto, H. *Inorg. Chem.* **1991**, *30*, 3575. Ni: (h) Feliz, M.; Llusar, R.; Uriel, S.; Vicent, C.; Brorson, M.; Herbst, K. *Polyhedron* **2005**, *10*, 1212.
(6) (a) Takei, I.; Dohki, K.; Kobayashi, K.; Suzuki, T.; Hidai, M. *Inorg. Chem.* **2005**, *44*, 3768. (b) Takei, I.; Wakebe, Y.; Suzuki, K.; Enta, Y.; Suzuki, T.; Mizobe, Y.; Hidai, M. *Organometallics* **2003**, *22*, 4639. (c) Herbst, K.; Monari, M.; Brorson, M. *Inorg. Chem.* **2002**, *41*, 1336. (d) Wakabayashi, T.; Ishii, Y.; Ishikawa, K.; Hidai, M. *Angew. Chem., Int. Ed.* **1996**, *18*, 2123. (e) Taniguchi, M.; Imamura, D.; Ishige, H.; Ishii, Y.; Murata, T.; Hidai, M.; Tatsumi, T. *J. Catal.* **1999**, *187*, 139. (f) Wakabayashi, T.; Ishii, Y.; Murata, T.; Mizobe, Y.; Hidai, M. *Tetrahedron Lett.* **1995**, *36*, 5585.
(7) Trofimenko, S. *Scorpionates*: *The Coordination Chemistry of Polypyrazolylborate Ligands*; Imperial College; London, 1999.
(8) Cotton, F. A.; Llusar, R.; Schwotzer, W. *Inorg. Chim. Acta* **1989**, *155*, 231.

a 74% yield (147 mg). Anal. Calcd for $C_{27}H_{32}B_3F_6Mo_3N_{18}PO_2S_3$: C, 26.98; H, 2.68; N, 20.97. Found: C, 27.10; H, 2.03; N, 20.93. ^{1}H NMR (CD_2Cl_2, −40 °C): δ 5.14 (d, 1H), 5.66 (t, 1H), 5.90 (c, 2H), 6.00 (d, 1H), 6.13 (d, 1H), 6.18 (t, 1H), 6.25 (t, 1H), 6.40 (t, 1H), 6.51 (t, 1H), 6.53 (t, 1H), 6.66 (d, 1H), 7.64 (d, 1H), 7.77 (d, 1H), 7.78 (s, 2H), 7.84 (d, 1H), 7.95 (d, 1H), 8.08 (d, 1H), 8.11 (s, 2H), 8.13 (d, 1H), 8.16 (t, 2H), 8.25 (t, 2H), 8.38 (d, 1H).

Syntheses of Sulfur-Bridged Cubane-Type Mo−Fe Clusters with Tp Ligands. All the experiments were carried out under a dinitrogen atmosphere.

[5]·4.5CH$_2$Cl$_2$ (fw 1528.66). An iron powder[9] (229.2 mg, 4.1 mmol) and tetrabutylammonium chloride (113.9 mg, 0.41 mmol) were added to a dichloromethane solution (40 mL) containing [**3**]-PF_6·H_2O (100 mg, 0.08 mmol). The mixture was stirred for 3 days. After the remaining iron was removed, the resultant solution was concentrated to 1/5 of its original volume and kept at room temperature. Black-purple crystals of [**5**]·4.5CH_2Cl_2 were deposited in a few days. Yield: 76 mg, 61%. Anal. Calcd for $C_{28}H_{32}B_3Cl_3$-$FeMo_3N_{18}S_4$: C, 27.31; H, 2.62; N, 20.47. Found: C, 26.97; H, 2.35; N, 20.46.

[6]·4.5CH$_2$Cl$_2$ (fw 1573.11), An iron powder[9] (229.2 mg, 4.1 mmol) and tetraetylammonium bromide (TEABr, 86.2 mg, 0.41 mmol) were added to a dichloromethane solution (40 mL) containing [**3**]PF_6·H_2O (100 mg, 0.08 mmol). The mixture was stirred for 3 days. After the remaining iron was removed, the resultant solution was concentrated to 1/5 of its original volume and kept at room temperature. Black-purple crystals of [**6**]·4.5CH_2Cl_2 were deposited in a few days. Yield: 39 mg, 41%. Anal. Calcd for $C_{27}H_{30}B_3$-$BrFeMo_3N_{18}S_4$: C, 27.23; H, 2.54; N, 21.17. Found: C, 27.64; H, 2.55; N, 20.99.

X-ray Crystallography for [3]Cl·4H$_2$O, [4]PF$_6$·H$_2$O, [5]·4.5CH$_2$Cl$_2$, and [6]·4.5CH$_2$Cl$_2$. Crystals of [**3**]Cl·4H_2O, [**4**]PF_6·H_2O, [**5**]·4.5CH_2Cl_2, and [**6**]·4.5CH_2Cl_2 suitable for the X-ray crystallography were covered with vacuum grease and mounted in a cryoloop (Hampton Research Corp.). Data collection for each crystal was performed (at 93 K) on a Rigaku RAXIS-IV two-dimensional detector equipped with a low-temperature apparatus using Mo Kα radiation (λ = 0.71073 Å). Empirical absorption corrections were applied using the program ABSCOR.[10] The structures of the compounds were solved by direct methods (SHELX 97[11]) with the aid of successive difference Fourier maps and refined with the full-matrix least-squares method on F^2. The Cl atom in [**3**]Cl·4H_2O and the dichloromethane molecules in [**5**]·4.5CH_2Cl_2 and [**6**]·4.5CH_2Cl_2 were disordered. Refinement of the disordered atom and molecules was performed so that the temperature factor for each atom might become equal for every element. The statistical disorder between two μ-S atoms and a μ-O atom was observed in the structure of [**4**]PF_6·H_2O. The occupancy factors of the μ-S and μ-O atoms were fixed at 2/3 and 1/3, respectively. All hydrogen atoms were included in the refinement at calculated positions, riding on their carrier atoms (C−H and B−H = 0.95 Å). The isotropic thermal parameters of the hydrogen atoms were constrained to 1.2U_{eq}, to which they were attached. The final difference Fourier maps showed no significant electron density. All calculations were performed with the program package Crystal Structure 3.6.0[12]

Electronic Spectroscopy. Electronic spectra (400∼1100 nm) of [**3**]PF_6·H_2O, [**4**]PF_6·H_2O, and [**5**]·4.5CH_2Cl_2 in CH_2Cl_2 were measured on a Hitachi U-2000 spectrophotometer.

Electrochemistry. Cyclic voltammetric measurements of [**5**]·4.5CH_2Cl_2 (0.5 mM) were performed in a 0.1 M dichloromethane solution of tetrabuthylammonium hexafluorophosphate on a BAS100W with a glassy carbon working electrode, an Ag/AgCl reference electrode, and platinum wire counter electrode. The redox potential of the $Fe(C_5H_5)_2/Fe(C_5H_5)_2^+$ couple was +0.19 V with respect to this reference electrode.

^{1}H NMR and HH COSY Spectra of 3 and 4. ^{1}H NMR and HH COSY spectra of **3** and **4** were obtained in 5 mm o.d. NMR tubes on a Bruker ARX-NMR spectrometer operating at 400 MHz. The samples were prepared by dissolving each compound ([**3**]BF_4·2H_2O, ca. 13 mg; [**4**]PF_6·H_2O, ca. 20 mg) in 0.75 mL of CD_2Cl_2. Proton chemical shifts were measured relative to the CD_2Cl_2 solvent peak (5.33 ppm). All the ^{1}H NMR and HHCOSY data were obtained at 233−323 K.

Results and Discussion

Designations of Complexes.

$[Mo_3S_4(H_2O)_9]^{4+}$	**1**
$[Mo_3OS_3(H_2O)_9]^{4+}$	**2**
$[Mo_3S_4Tp_3]^+$	**3**
$[Mo_3OS_3Tp_3]^+$	**4**
$[Mo_3FeS_4ClTp_3]$	**5**
$[Mo_3FeS_4BrTp_3]$	**6**
$[\{Mo_3S_4Tp_2\}_2(\mu\text{-O})(\mu\text{-pz})_2]$	**7**
$[Mo_3FeS_4(H_2O)_{10}]^{4+}$	**8**

Syntheses of [3]Cl·4H$_2$O, [3]tof·2H$_2$O, [3]PF$_6$·H$_2$O, [3]BF$_4$·2H$_2$O, [4]PF$_6$·H$_2$O, [5]·4.5CH$_2$Cl$_2$, and [6]·4.5CH$_2$Cl$_2$. The reaction of $[Mo_3S_4(H_2O)_9]^{4+}$ (**1**) with KTp afforded [**3**]-Cl·4H_2O in an excellent yield. All the molybdenum atoms are bonded to the Tp ligand. Cotton and co-workers reported the preparation and an X-ray structure of $[\{Mo_3S_4Tp_2\}_2(\mu\text{-O})(\mu\text{-pz})_2]$ (**7**, pz = pyrazole),[8] They pointed out the KTp that they used contained a small amount of pyrazole as an impurity, and this led to the formation of **7**. We succeeded in obtaining only the target complex **3** with a high yield. While developing a new method to prepare complex **3**, we found that the existence of an excess amount of chloride anions led to decomposition of the ligand Tp in MeOH solution. We report four kinds of salts of **3**, [**3**]Cl·4H_2O, [**3**]-tof·2H_2O, [**3**]PF_6·H_2O, and [**3**]BF_4·2H_2O in this paper. The solubility and stability of the chloride salt in organic solvents differ completely from those of the other salts: (1) [**3**]Cl·4H_2O dissolves well in MeOH and is stable in the air, while the other salts do not dissolve in the solvent. (2) [**3**]Cl·4H_2O dissolves in acetonitrile, acetone, and dichloromethane, and the solutions are unstable even under dinitrogen atmosphere,[13] while the other salts dissolve well in the solvents and are stable in the air. The addition of tetrabutylammonium

(9) Iron powder washed with HCl, rinsed with water and CH_2Cl_2, and dried.
(10) Higashi, T., *ABSCOR;* RIGAKU Corporation: Tokyo, Japan.
(11) Sheldrick, G. M. *SHELX97*; University of Göttingen: Göttingen, Germany, 1997.
(12) *CrystalStructure 3.6.0*: *Crystal Structure Analysis Package*; Rigaku and Rigaku/MSC: The Woodlands, TX, 2000−2004.
(13) CH_3CN and CH_2Cl_2 solutions of [**3**]Cl·4H_2O were stable at low temperature (below 0 °C).

Table 1. Crystallographic Data for [**3**]Cl·4H_2O, [**4**]PF_6·H_2O, [**5**]·4.5CH_2Cl_2, and [**6**]·4.5CH_2Cl_2

	[**3**]Cl·4H_2O	[**4**]PF_6·H_2O	[**5**]·4.5CH_2Cl_2	[**6**]·4.5CH_2Cl_2
empirical formula	$C_{27}H_{38}B_3ClMo_3N_{18}O_4S_4$	$C_{27}H_{30}B_3F_6Mo_3N_{18}O_2PS_3$	$C_{31.5}H_{39}B_3Cl_{10}FeMo_3N_{18}S_4$	$C_{31.5}H_{39}B_3BrCl_9FeMo_3N_{18}S_4$
fw	1162.66	1200.06	1528.64	1573.09
cryst syst	trigonal	trigonal	trigonal	trigonal
a (Å)	14.7494(9)	15.121(1)	17.5965(7)	17.6869(3)
c (Å)	33.752(2)	32.755(3)	61.372(3)	61.428(1)
V (Å^3)	6358.8(7)	6485(1)	16457.0(11)	16641.9(5)
T (K)	93	93	93	93
space group	$R\bar{3}$ (No. 148)	$R\bar{3}$ (No. 148)	$R\bar{3}$ (No. 148)	$R\bar{3}$ (No. 148)
Z	6	6	12	12
μ(Mo Kα) (cm^{-1})	11.91	11.16	16.13	22.7
reflns collected	14 045	12 590	37 394	41 185
unique reflns	3193 (R_{int} = 0.053)	3273 (R_{int} = 0.051)	8052 (R_{int} = 0.044)	8355 (R_{int} = 0.081)
R1, wR2 (all data)	0.076, 0.161	0.120, 0.198	0.089, 0.191	0.117, 0.198
R1 ($I > 2.00\sigma(I)$)	0.065	0.072	0.073	0.075

chloride to a dichloromethane solution of [**3**]tof·2H_2O or [**3**]-PF_6·H_2O caused an immediate decomposition of the compound. The existence of the chloride ion may be the cause of the decomposition of the compound in aprotic solvents. Still, it is not clear why the stability of **3** in MeOH differs significantly from that of **3** in aprotic solvents. We consider the possibility that cluster **3** seems to be stabilized by the hydrogen bond between an oxygen atom of methanol and the hydrogen atom attached to the boron atom in the Tp ligand. An anion exchange reaction of [**3**]Cl·4H_2O in MeOH can be used to isolate the [**3**]tof·2H_2O, [**3**]PF_6·H_2O, and [**3**]-BF_4·2H_2O as insoluble microcrystals by taking advantage of the solubility difference of the salts. Electronic spectra of these compounds are the same in dichloromethane and indistinguishable from that of [**3**]Cl·4H_2O in MeOH, regardless of the counteranion.

We have also prepared a new compound, [**4**]PF_6·H_2O, from the reaction of **2** with KTp in the presence of NH_4PF_6. All the molybdenum atoms are bonded to the Tp ligand. To prevent a decomposition reaction of the Tp ligand, NH_4PF_6 was added to the solution to remove the chloride ion as NH_4-Cl (eq 1). The color of the reaction mixture in MeOH changed to brown without NH_4PF_6, indicating decomposition of cluster **4**.

$$[Mo_3OS_3Cl_4(H_2O)_5] + 4NH_4PF_6 + 4H_2O \rightarrow [Mo_3OS_3(H_2O)_9](PF_6)_4 + 4NH_4Cl\downarrow \quad (1a)$$

$$[Mo_3OS_3(H_2O)_9](PF_6)_4 + 3KTp \xrightarrow{MeOH} [Mo_3OS_3Tp_3]PF_6\ ([\mathbf{4}](PF_6)) + 3KPF_6 + 9H_2O \quad (1b)$$

The reaction of **3** with metallic iron in CH_2Cl_2 produced $[Mo_3FeS_4ClTp_3]$ (**5**) (eq 2). Also, $[Mo_3FeS_4BrTp_3]$ (**6**) was prepared by a method similar to that of **5**, using TEABr.

$$[Mo_3S_4Tp_3]PF_6\ ([\mathbf{3}]PF_6) + Fe + TBACl \rightarrow [Mo_3FeS_4ClTp_3]\ (\mathbf{5}) + TBAPF_6 \quad (2)$$

The iron insertion reaction into the Mo_3S_4 core of **3** is a reductive addition as in the case of the metal insertion reaction of **1** in aqueous solutions (the formal oxidation states of the molybdenum and iron atoms in **5** changed from Mo_3^{IV} and Fe^0 to $Mo^{IV}Mo_2^{III}$ and Fe^{II}).[2a,2b] It is clear that the reducing power of the iron in a nonaqueous solvent is an important factor determining if the reaction proceeds.

Table 2. Selected Bond Lengths (Å) and Angles (deg) for [**3**]Cl·4H_2O[a]

atom	atom	length	atom	atom	length
Mo(1)	Mo(1)^1	2.832(1)	Mo(1)	S(1)	2.358(2)
Mo(1)	S(2)	2.295(2)	Mo(1)	N(1)	2.217(6)
Mo(1)	N(3)	2.207(5)	Mo(1)	N(5)	2.327(4)

atom	atom	atom	angle	atom	atom	atom	angle
Mo(1)^1	Mo(1)	Mo(1)^2	60.00(2)	S(1)	Mo(1)	S(2)	103.08(6)
S(2)	Mo(1)	S(2)^2	98.25(5)	S(1)	Mo(1)	N(1)	168.2(1)
S(1)	Mo(1)	N(3)	82.8(1)	S(1)	Mo(1)	N(5)	99.7(1)
S(2)	Mo(1)	N(1)	87.4(1)	S(2)	Mo(1)	N(3)	157.8(1)
S(2)	Mo(1)	N(5)	81.5(1)	N(1)	Mo(1)	N(3)	85.4(2)
N(1)	Mo(1)	N(5)	76.1(2)	N(3)	Mo(1)	N(5)	76.3(2)
Mo(1)	S(1)	Mo(1)^1	73.80(6)	Mo(1)	S(2)	Mo(1)^1	76.64(5)

[a] Symmetry operators: (1) $-y + 1, x - y + 1, z$; (2) $-x + y, -x + 1, z$.

Complexes **5** and **6** represent the first examples of cubane-type molybdenum−iron clusters prepared from **3** and metallic iron in nonaqueous solvents.

It became clear that complex **3** functions as a metal-complex ligand for the preparation of a novel mixed-metal complex even in nonaqueous solvents. We have prepared the clusters with Mo_3MS_4 (M = Ni, Pd, Pt, Cu) cores using **3** as the starting complex. Characterizations of the clusters in more detail are currently under investigation and will be reported elsewhere. In contrast to **3**, cluster **4** does not react with iron to produce a mixed-metal cubane-type sulfide cluster containing a Mo_3FeOS_3 core.

X-ray Crystallography. Crystallographic and refinement data for [**3**]Cl·4H_2O, [**4**]PF_6·H_2O, [**5**]·4.5CH_2Cl_2, and [**6**]·4.5CH_2Cl_2 are summarized in Table 1. Selected bond distances and angles for [**3**]Cl·4H_2O, [**4**]PF_6·H_2O, [**5**]·4.5CH_2Cl_2, and [**6**]·4.5CH_2Cl_2 are listed in Tables 2−5, respectively, and ORTEP drawings of clusters **3**, **4**, and **5** are shown in Figures 1−3, respectively.

Clusters **3**, **5**, and **6** have a crystallographic C_3 symmetry, with a μ_3-S (S1) atom on a 3-fold axis (Fe and Cl atoms in **5** and Fe and Br atoms in **6** also lie on the 3-fold axis). For [**4**]PF_6·H_2O, statistical disorder was observed between two μ-S and one μ-O atoms to give a crystallographic 3-fold axis. The μ-S and μ-O atoms were refined with a partial occupancies of 2/3 and 1/3, respectively. Only the two μ-S atoms and one μ-O atom are included in the ORTEP drawing of **4** for clarity.

The dichloromethane molecules show severe disorder in [**5**]·4.5CH_2Cl_2 and [**6**]·4.5CH_2Cl_2. The structure of [**6**]·

Table 3. Selected Bond Lengths (Å) and Angles (deg) for [**4**]PF_6·H_2O[a]

atom	atom	length	atom	atom	length
Mo(1)	Mo(1)[1]	2.676(1)	Mo(1)	S(1)	2.305(2)
Mo(1)	S(2)	2.316(6)	Mo(1)	S(2)[1]	2.266(6)
Mo(1)	O(1)	1.77(3)	Mo(1)	O(1)[1]	1.82(2)
Mo(1)	N(1)	2.147(7)	Mo(1)	N(3)	2.131(8)
Mo(1)	N(5)	2.227(9)			

atom	atom	atom	angle	atom	atom	atom	angle
S(1)	Mo(1)	S(2)	105.9(1)	S(1)	Mo(1)	O(1)	96.7(6)
S(1)	Mo(1)	N(1)	166.6(2)	S(1)	Mo(1)	N(3)	79.8(2)
S(1)	Mo(1)	N(5)	98.7(2)	S(2)	Mo(1)	S(2)[1]	100.6(2)
S(2)	Mo(1)	O(1)[1]	95.2(8)	S(2)	Mo(1)	N(1)	86.6(3)
S(2)	Mo(1)	N(3)	154.3(3)	S(2)	Mo(1)	N(5)	77.0(3)
O(1)	Mo(1)	N(1)	96.5(6)	O(1)	Mo(1)	N(3)	163.4(7)
O(1)	Mo(1)	N(5)	87.1(7)	N(1)	Mo(1)	N(3)	86.8(3)
N(1)	Mo(1)	N(5)	79.1(3)	N(3)	Mo(1)	N(5)	77.4(4)
Mo(1)	S(1)	Mo(1)[1]	70.97(8)	Mo(1)	S(2)	Mo(1)[2]	71.5(1)
Mo(1)	O(1)	Mo(1)[2]	96.3(8)				

[a] Symmetry operators: (1) $-y, x-y, z$; (2) $-x+y, -x, z$.

Table 4. Selected Bond Lengths (Å) and Angles (deg) for [**5**]·$4.5CH_2Cl_2$[a]

atom	atom	length	atom	atom	length
Mo(1)	Mo(1)[1]	2.8893(7)	Mo(1)	Fe(1)	2.731(2)
Mo(1)	S(1)	2.373(2)	Mo(1)	S(2)	2.330(2)
Mo(1)	N(1)	2.247(6)	Mo(1)	N(3)	2.236(5)
Mo(1)	N(5)	2.301(8)	Fe(1)	Cl(1)	2.235(4)
Fe(1)	S(2)	2.226(2)			

atom	atom	atom	angle	atom	atom	atom	angle
Mo(1)[1]	Mo(1)	Mo(1)[3]	60.00(2)	Mo(1)[1]	Mo(1)	Fe(1)	58.07(3)
Mo(1)[1]	Mo(1)	S(1)	52.50(4)	Mo(1)[1]	Mo(1)	S(2)	52.25(5)
Mo(1)[1]	Mo(1)	N(1)	140.7(1)	Mo(1)[1]	Mo(1)	N(3)	134.0(1)
Mo(1)[1]	Mo(1)	N(5)	101.1(1)	Fe(1)	Mo(1)	S(1)	97.69(6)
Fe(1)	Mo(1)	S(2)	51.43(6)	Fe(1)	Mo(1)	N(1)	93.7(2)
Fe(1)	Mo(1)	N(3)	148.8(2)	Fe(1)	Mo(1)	N(5)	131.9(2)
S(1)	Mo(1)	S(2)	103.30(6)	S(1)	Mo(1)	N(1)	166.7(2)
S(1)	Mo(1)	N(3)	82.1(2)	S(1)	Mo(1)	N(5)	100.3(2)
S(2)	Mo(1)	S(2)[2]	100.35(7)	S(2)	Mo(1)	N(1)	89.2(2)
S(2)	Mo(1)	N(3)	159.1(2)	S(2)	Mo(1)	N(5)	81.0(2)
N(1)	Mo(1)	N(3)	84.6(2)	N(1)	Mo(1)	N(5)	76.8(2)
N(3)	Mo(1)	N(5)	78.1(3)	Mo(1)	Fe(1)	Mo(1)[1]	63.87(4)
Mo(1)	Fe(1)	Cl(1)	142.36(3)	Mo(1)	Fe(1)	S(2)	54.93(6)
S(2)	Fe(1)	S(2)[1]	107.77(9)	Cl(1)	Fe(1)	S(2)	111.12(7)
Mo(1)	S(1)	Mo(1)[1]	75.01(8)	Mo(1)	S(2)	Mo(1)[1]	76.20(7)
Mo(1)	S(2)	Fe(1)	73.64(8)				

[a] Symmetry operators: (1) $-y+1, x-y, z$; (2) $-y+1, x-y-1, z$; (3) $-x+y+1, -x+1, z$.

$4.5CH_2Cl_2$ is similar to that found in [**5**]·$4.5CH_2Cl_2$, except that the Br^- anion attached to the iron atom in the Mo_3FeS_4 core. In the case of [**5**]·$4.5CH_2Cl_2$ and [**6**]·$4.5CH_2Cl_2$, the unit cell has two independent chemical units, but no significant structural difference can be seen between the two units. For this reason, only the selected bond distances and angles of one side of the two independent molecules are shown in Tables 4 and 5.

The replacement of aqua ligands of **1** by Tp molecules leads to the elongation of Mo−Mo distances in **3**. The Mo−Mo, Mo−μ-S, and Mo−μ_3-S distances in analogous complexes with $Mo^{IV}{}_3S_4$ cores are listed in Table 6. Cluster **3** has the longest Mo−Mo distances among the complexes, probably because of the electron donating ability of Tp ligands. Similar effects are observed with the Mo−Mo distances in $[\{Mo_3S_4Tp_2\}_2(\mu\text{-O})(\mu\text{-pz})_2]$·2THF[8] and

Table 5. Selected Bond Lengths (Å) and Angles (deg) for [**6**]·$4.5CH_2Cl_2$[a]

atom	atom	length	atom	atom	length
Mo(1)	Mo(1)[1]	2.899(1)	Mo(1)	Fe(1)	2.722(3)
Mo(1)	S(1)	2.373(3)	Mo(1)	S(2)	2.330(2)
Mo(1)	N(1)	2.25(1)	Mo(1)	N(3)	2.235(9)
Mo(1)	N(5)	2.308(8)	Br(1)	Fe(1)	2.334(4)
Fe(1)	S(2)	2.235(2)			

atom	atom	atom	angle	atom	atom	atom	angle
Mo(1)[1]	Mo(1)	Mo(1)[2]	60.00(3)	Mo(1)[1]	Mo(1)	Fe(1)	57.81(4)
Mo(1)[1]	Mo(1)	S(1)	52.34(6)	Mo(1)[1]	Mo(1)	S(2)	51.35(7)
Mo(1)[1]	Mo(1)	N(1)	140.7(2)	Mo(1)[1]	Mo(1)	N(3)	134.1(2)
Mo(1)[1]	Mo(1)	N(5)	101.1(2)	Fe(1)	Mo(1)	S(1)	97.16(9)
Fe(1)	Mo(1)	S(2)	51.82(6)	Fe(1)	Mo(1)	N(1)	94.1(3)
Fe(1)	Mo(1)	N(3)	148.8(2)	Fe(1)	Mo(1)	N(5)	131.8(2)
S(1)	Mo(1)	S(2)	103.15(9)	S(1)	Mo(1)	N(1)	166.8(2)
S(1)	Mo(1)	N(3)	82.3(3)	S(1)	Mo(1)	N(5)	100.7(2)
S(2)	Mo(1)	S(2)[2)]	100.98(9)	S(2)	Mo(1)	N(1)	89.2(2)
S(2)	Mo(1)	N(3)	158.7(2)	S(2)	Mo(1)	N(5)	80.6(2)
N(1)	Mo(1)	N(3)	84.5(3)	N(1)	Mo(1)	N(5)	76.6(3)
N(3)	Mo(1)	N(5)	78.2(3)	Mo(1)	Fe(1)	Mo(1)[1]	64.38(7)
Mo(1)	Fe(1)	Br(1)	142.04(4)	Mo(1)	Fe(1)	S(2)	55.03(8)
Br(1)	Fe(1)	S(2)	110.8(1)	S(2)	Fe(1)	S(2)[1]	108.1(1)
Mo(1)	S(1)	Mo(1)[1]	75.3(1)	Mo(1)	S(2)	Mo(1)[1]	76.34(8)
Mo(1)	S(2)	Fe(1)	73.15(8)				

[a] Symmetry operators: (1) $-y+1, x-y, z$; (2) $-y+1, x-y-1, z$.

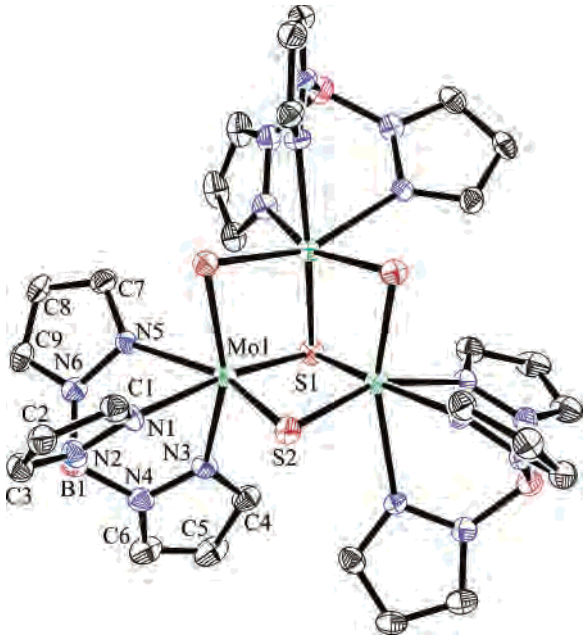

Figure 1. ORTEP diagram of **3**.

$[Mo_3Cp_3S_4][Sn(CH_3)_3Cl_2]$.[14] There are no significant differences in the Mo−S distances among the compounds listed in Table 6.

If the Mo−Mo bonds are ignored, each molybdenum atom has a six-coordinated distorted-octahedral geometry in **3**. Steric hindrance between the ligands' Tp units may be the cause of the distortion. A projection of compound **3** down the B1−Mo1 axis is shown in Figure 4, where only the crystallographically independent atoms are shown except for

(14) Vergarmini, P. J.; Vahrenkamp, H.; Dahl, L. F. *J. Am. Chem. Soc.* **1971**, *93*, 6327.

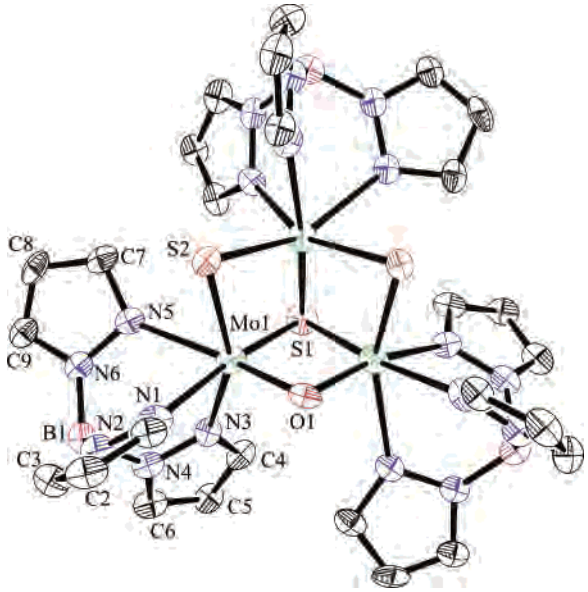

Figure 2. ORTEP diagram of **4**.

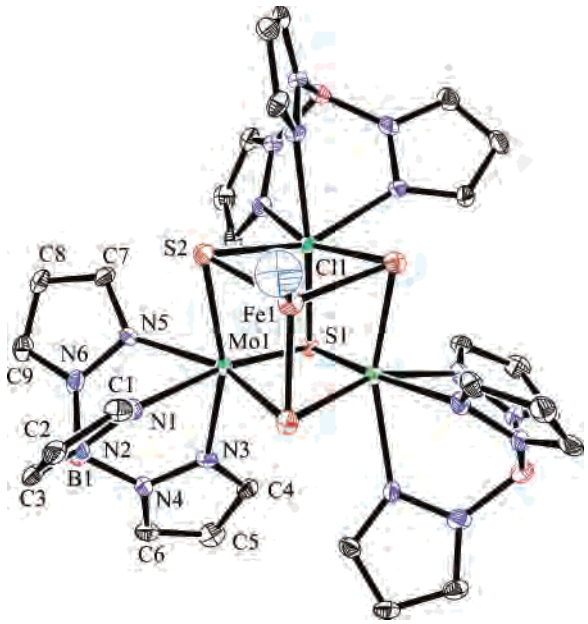

Figure 3. ORTEP diagram of **5**.

the Mo1[a], S2[a], Mo1[b], and S2[b] atoms (symmetry operators: a $-x + y, -x, z$; b $-y, +x - y, x$).

The dihedral angle between pyrazole rings **a** (N1, N2, C1, C2, C3) and **b** (N3, N4, C4, C5, C6) is 144.5°, whereas the dihedral angle between pyrazole rings **a** (N1, N2, C1, C2, C3) and **c** (N5, N6, C7, C8, C9) is far smaller (98.1°). Therefore, pyrazole ring **b** is under pyrazole ring **c′**, which is coordinated to the adjacent molybdenum atom, so that pyrazole rings **b** and **c′** have less steric hindrance. The distortion of the structure of the Tp ligand was also confirmed from the analysis of the ^{1}H NMR spectrum of **3**. Such distorted octahedral geometries around the molybdenum atoms are also observed in **4**, **5**, and **6**.

The Mo1−N5 (2.327(4) Å) distance in **3** is 0.1 Å longer than the other Mo−N distances (Mo1−N1 = 2.217(6) Å, Mo1−N3 = 2.207(5) Å). Similar tendencies are observed for the Mo−N distances in **4**, **5**, **6**, **7**, and [$Mo_4S_4Tp_4(\mu$-pz)],[23] while the Mo−N distances do not vary widely in multinuclear metal compounds with one Tp ligand.[24] The steric hindrance between the Tp ligands may be the cause of the scattered Mo−N distances in the multinuclear compounds.

The Mo−Mo distances (2.8893(7) Å) in **5** are ca. 0.12 Å longer than the Mo−Mo distances (2.767[7] Å) in **8**.[2b] The elongation seems to be the result of the electron donating property of the Tp ligands. There are no significant differences in the Mo−Fe distances in **5** and **8**.[2b]

Table 6. Comparison of Mo−Mo and Mo−S Distances (Å) in Incomplete Cubane-Type Compounds with Mo_3S_4 Cores[a]

	Mo−Mo	Mo−μ_3-S	Mo−μ-S
$[Mo_3S_4Tp_3]Cl\cdot 4H_2O$	2.8314(3)	2.3576(8)	2.2689(8)
$[\{Mo_3S_4Tp_2\}_2(O)(pz)_2]\cdot 2THF$[8]	2.830(24)	2.352(11)	2.292(22)
$[Mo_3S_4Cp_3][Sn(CH_3)_3Cl_2]$[14]	2.812(1)	2.314(6)	2.294(6)
$[Mo_3S_4Cl_4(PEt_3)_4(MeOH)]$[15]	2.790(5)	2.359(8)	2.289(23)
$[(C_2H_5)_4N]_2[Mo_3S_4(SCH_2CH_2S)_3]$[16]	2.783(12)	2.345(3)	2.293(22)
$K_5[Mo_3S_4(CN)_9]\cdot 7H_2O$[17]	2.765(7)	2.363(4)	2.312(5)
$[Mo_3S_4(dtp)_4(H_2O)]$[18]	2.754(18)	2.346(9)	2.281(19)
$Na_2[Mo_3S_4(Hnta)_3]\cdot 5H_2O$[19]	2.754(18)	2.334(4)	2.290(13)
$Ca[Mo_3S_4(ida)_3]\cdot 11.5H_2O$[20]	2.754(11)	2.348(9)	2.294(8)
$[Mo_3S_4(dtc)_4(dmf)]\cdot EtOH$[21]	2.741(38)	2.336(3)	2.297(3)
$Cs[Mo_3S_4(ox)_3(H_2O)_3]\cdot 3H_2O$[22]	2.738(5)	2.33(1)	2.28(1)
$[Mo_3S_4(H_2O)_9](pts)_4\cdot 9H_2O$[1d]	2.732(7)	2.332(4)	2.286(6)

[a] Abbreviations: Cp = C_5H_5, dtp = $(C_2H_5)_2PS_2$, Hnta = $N(CH_2CO_2)_3H^{2-}$, ida = $HN(CH_2CO_2)_2^{2-}$, dtc = $(C_2H_5)_2NCS_2^-$, ox = $C_2O_4^{2-}$.

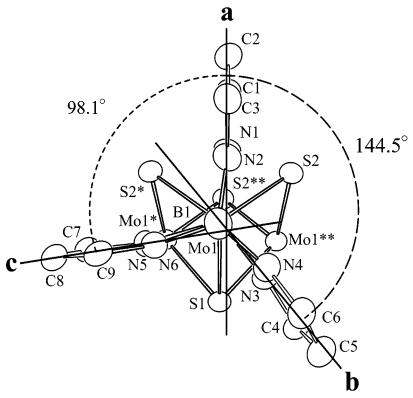

Figure 4. ORTEP plot showing the angles of between each plane (*a*, *b*, and *c*).

(15) Saito, T.; Yamamoto, N.; Yamanaga, T.; Imoto, H. *Chem. Lett.* **1987**, 2025.
(16) Halbet, T. R.; McGauley, K.; Pan, W. H.; Czernuszewicz, R. S.; Stiefel, E. I. *J. Am. Chem. Soc.* **1984**, *106*, 1849.
(17) Howlader, N. C.; Haight, G. P., Jr.; Hambley, T. W.; Lawrance, G. A.; Rahmoeller, K. M.; Snow, M. R. *Aust. J. Chem.* **1983**, *36*, 377.
(18) (a) Huang, J. Q.; Huang, J. L.; Shang, M. Y.; Lu, S. F.; Lin, X. T.; Lin, Y. H.; Huang, M. D.; Zhuang, H. H.; Lu, J. X. *Pure Appl. Chem.* **1988**, *60*, 1185. (b) Lin, X.; Lin, Y.; Huang, J.; Huang, J. *Kekue Tongbao* **1987**, *32*, 810.
(19) Yamsaki, M.; Shibahara, T. *Anal. Sci.* **1992**, *8*, 727.
(20) Shibahara, T.; Kuroya, H. *Polyhedron* **1986**, *5*, 357.
(21) Huang, M.-D.; Lu, S.-F.; Huang, J.-Q.; Huang, J.-L. *Acta Chim. Sin.* **1989**, *47*, 121.
(22) (a) Cotton, F. A.; Llusar, R. *Polyhedron* **1987**, *6*, 1741. (b) Cotton, F. A.; Dori, Z.; Llusar, R.; Schwotzer, W. *J. Am. Chem. Soc.* **1985**, *107*, 6734.
(23) Cotton, F. A.; Dori, Z.; Llusar, R.; Schwotzer, W. *Inorg. Chem.* **1986**, *25*, 3529.
(24) For example, see: Fomitchev, D. V.; McLauchlan, C. C.; Holm, R. H. *Inorg. Chem.* **2002**, *41*, 951.

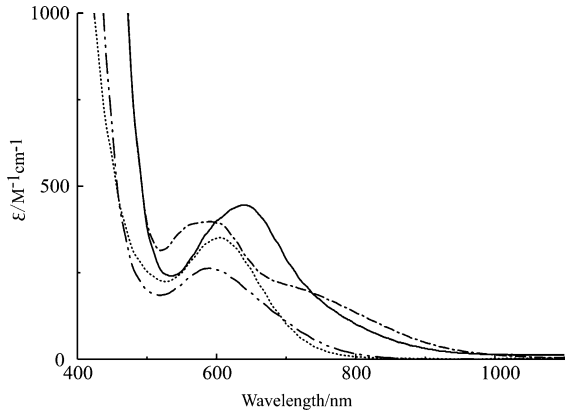

Figure 5. UV−vis spectra of **3** in CH_2Cl_2 (—), **4** in CH_2Cl_2 (- · -), **1** in an aqueous solution of 2 M Hpts (- - -), and **2** in an aqueous solution of 2 M Hpts (- · · -).

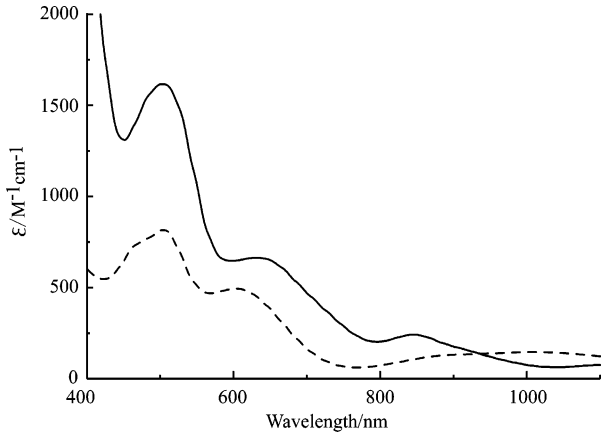

Figure 6. UV−vis spectra of **5** in CH_2Cl_2 (—) and **8** in an aqueous solution of 2 M Hpts (- - -).

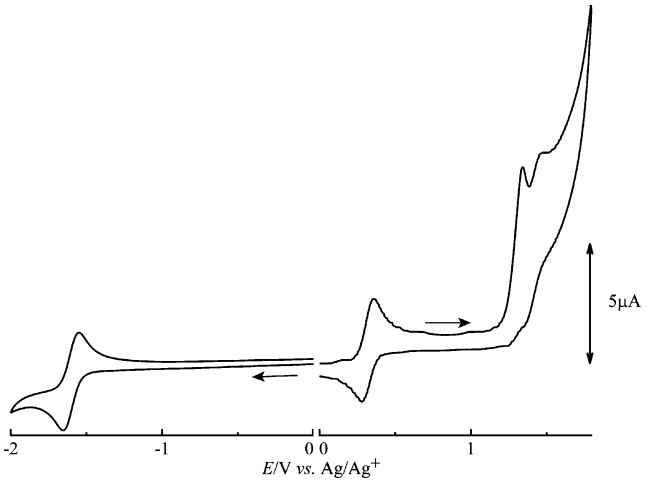

Figure 7. Cyclic voltammograms of [**5**]·$4.5CH_2Cl_2$ (0.5 mM) in CH_2Cl_2 containing 0.1 M $TBAPF_6$ (scan rate = 100 mV s^{-1}).

No significant difference in the Mo−Mo bond distances can be seen between the Mo_3OS_3 moieties in **4** and $[Mo_3OS_3(H_2O)_9](pts)_4 \cdot 7H_2O$ ([**2**](pts)$_4$·$7H_2O$, pts = *p*-toluenesulfonate).[25] Thus, it is clear that the replacement of aqua ligands in **2** by Tp molecules does not lead to the elongation of the Mo−Mo distances in [**4**]$PF_6 \cdot H_2O$. The Mo−μ-O distances (1.77(3) and 1.82(2) Å) in **4** are shorter than those observed in [**2**](pts)$_4$·$7H_2O$ (2.150(3) and 2.129(4) Å), but the disorder in **4** prevents us from further discussion.

Electronic Spectroscopy. Figure 5 shows the electronic spectra of [**3**]$PF_6 \cdot H_2O$ [λ_{max} (ϵ) = 640 nm (445 M^{-1} cm^{-1})] and [**4**]$PF_6 \cdot H_2O$ [λ_{max} (ϵ) = 590 nm (395 M^{-1} cm^{-1})] in CH_2Cl_2 together with those of **1** and **2** in 2 M Hpts. The characteristic peak position for **3** appeared at a longer wavelength of 640 nm compared to that of aqua cluster **1**. This observation is consistent with the fact that the nine water molecules attached to the molybdenum atoms were substituted with three electron-donating Tp ligands. The dichloromethane solution of [**3**]$PF_6 \cdot H_2O$ is air-stable.

The spectrum of **4** shows three broad peaks in the visible region, while that of **3** has only one peak in that region. This change may be caused by the lowering of the symmetry in **4** through the substitution of one μ-O for one μ-S. The dichloromethane solution of [**4**]$PF_6 \cdot H_2O$ is air-stable. Figure 6 shows the electronic spectra of [**5**]·$4.5CH_2Cl_2$ [λ_{max} (ϵ) = 500 (1616), 630 (663), 845 nm (241 M^{-1} cm^{-1})] in CH_2Cl_2 together with **8** in 2 M Hpts. The spectrum of **5** is similar to that of **8**. This similarity and X-ray structure analysis support the presence of a heterometallic cubane-type cluster, $[Mo_3FeS_4ClTp_3]$, in the solution. In contrast to the solution of **8** in 2 M Hpts solution, which is very air-sensitive, the dichloromethane solution of **5** is air-stable. The spectrum of **6** is identical to that of **5** in dichloromethane.

Electrochemistry. Figure 7 shows a cyclic voltammogram of **5**. The cyclic voltammogram of **5** shows two reversible one-electron couples ($E_{1/2}$ = −1.40 and 0.52 V vs SCE) and two irreversible one-electron oxidation processes (E_{pc} = 1.54 and 1.66 V vs SCE). The oxidation processes of **5** were observed for the first time by replacing the aqua ligands of **8** with Tp. A formal oxidation state of $Mo^{IV}Mo^{III}_2Fe^{II}$ is assigned to the cubane-type Mo_3FeS_4 moiety in the same manner as in **8**.[2b] The wave of the reduction process ($E_{1/2}$ = −1.40 V) corresponds to the change of oxidation states of the molybdenum atoms in **5**: $Mo^{IV}Mo^{III}_2Fe^{II} \rightarrow Mo^{III}_3Fe^{II}$. Also, the first ($E_{1/2}$ = 0.52 V) and second (E_{pc} = 1.54 V) waves of the oxidation process correspond to the change of oxidation states of the molybdenum atoms in **5**: $Mo^{IV}Mo^{III}_2Fe^{II} \rightarrow Mo^{IV}_2Mo^{III}Fe^{II} \rightarrow Mo^{IV}_3Fe^{II}$. For the third oxidation peak (E_{pc} = 1.66 V), the peak current is highly dependent on the scan rate and is not proportional to the square root of the scan rate. These observations indicate that the successive chemical reaction has occurred after the second step of the oxidation process. The third oxidation peak corresponds to the oxidation of a reaction product of the reaction. Although the details of this chemical reaction are not clear for the moment, it is probable that the coordination bond between a nitrogen atom of the Tp ligand and a molybdenum atom in **5** is cleaved by the oxidation. [26]

^{1}H NMR Spectroscopy. The ^{1}H NMR spectra of [**3**]$BF_4 \cdot 2H_2O$ (A, B, and C) in CD_2Cl_2 are shown in Figure 8 together with the ^{1}H NMR spectrum of KTp (D). The hydrogen atoms

(25) Shibahara, T.; Sakane, G.; Mochida, S. *J. Am. Chem. Soc.* **1993**, *115*, 10408.

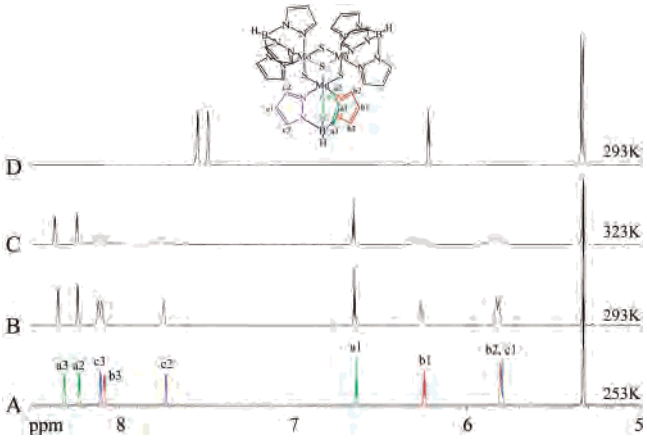

Figure 8. ^{1}H NMR spectra of [**3**]BF_4·$2H_2O$ (A, 253; B, 293; C, 323 K) and KTp (D, 293 K) in CD_2Cl_2 (400 MHz, CD_2Cl_2).

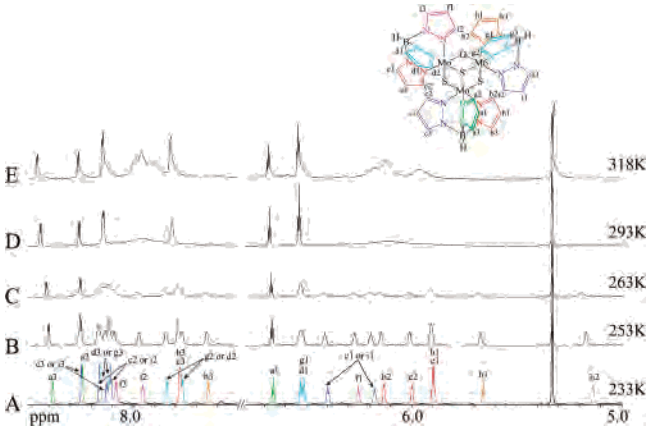

Figure 9. ^{1}H NMR spectra of [**4**]PF_6·H_2O in CD_2Cl_2 (A, 233; B, 253; C, 263; D, 293; E, 318 K; 400 MHz, CD_2Cl_2).

bound to the pyrazole rings of Tp have been identified as indicated in the inset of Figure 8. ^{1}H NMR signals corresponding to nine protons bonded to three pyrazole rings in one Tp were observed at 253 K (spectrum A). It shows that cluster **3** has a 3-fold rotation axis in CD_2Cl_2 solution; in other words, although all Tp ligands attached to each molybdenum atom are equivalent, three pyrazole rings in one Tp ligand have a different environment. The signals with which correlations were seen by the HH correlation spectrum of [**3**]BF_4·$2H_2O$ are shown in the same colors. All the signals were assigned as shown in Figure 8. The ^{1}H NMR spectra of [**3**]BF_4·$2H_2O$ at higher temperatures (B and C) show coalescence of the red and blue signals, while only the signal of Ha3 moves slightly to a lower magnetic field among the green signals. On the basis of the above observations, we think that an isomerization of **3** occurs in CD_2Cl_2 solution as shown in Scheme 2A. Since the environment of the protons on pyrazole ring **a** at the trans position to μ_3-S is not influenced by this isomerization reaction, the three green signals were assigned to Ha1, Ha2, and Ha3, as shown in Figure 8. The Hb2 signal of **3** appears at very high magnetic fields compared to the Ha2 or Hc2 signals. The MO calculation (Gaussian03 program package) of [**3**]BF_4·$2H_2O$ shows that the Mo−μ_3-S bonding orbital expands in the direction of Hb2, which may cause the upfield shift of the proton signal (see Supprting Information Figure 1).[27]

The ^{1}H NMR spectra of [**4**]PF_6·H_2O in CD_2Cl_2 are shown in Figure 9. Twenty-one ^{1}H NMR signals corresponding to twenty-seven protons bonded to nine pyrazole rings in three Tp ligands were observed at 233 K (spectrum A). The HH correlation spectrum of [**4**]PF_6·H_2O shows that nine pyrazole rings (**a**, **b**, **c**, **d**, **e**, **f**, **g**, **h**, and **i**) exist, as shown in the inset of Figure 9. Obviously, **4** has no 3-fold rotation axis, in contrast to **3**. All the signals were assigned to the corresponding hydrogen atom as shown in Figure 9. The ^{1}H NMR spectra of [**4**]PF_6·H_2O at higher temperatures (B and C) show coalescence of the signals at 6.5 ppm. Except for six ^{1}H NMR signals corresponding to nine protons, all other signals became broad at 293 K (spectrum D). New ^{1}H NMR signals appear near 6.1 and 8.0 ppm at 318 K (spectrum E). On the basis of the above observations, we think that an isomerization of **4** occurs in CD_2Cl_2 solution as shown in Scheme

Scheme 2

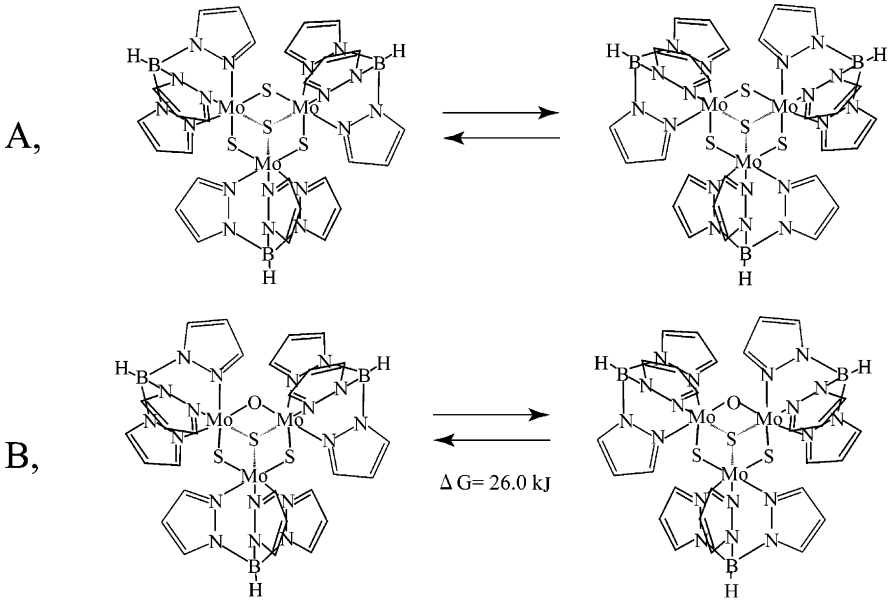

2B. The environment of protons on pyrazole rings **a**, **d**, and **g** at the trans position to μ_3-S is not influenced by the isomerization reaction. The three signals (green) were assigned to the protons attached to pyrazole ring **a**. The remaining six signals (light blue) can be divided into two groups (6.53 (1H, t), 7.84 (1H, d), 8.16 ppm (1H, d) and 6.51 (1H, t), 7.77 (1H, d), 8.11 ppm (1H, d)); however, the assignment of each set of signals to either pyrazole ring **d** or **g** is impossible. The Hb2, He2, and Hh2 signals of **4** appear at very high magnetic fields compared to the Ha2 signal. An optimized structure of **4** was calculated using the Gaussian03 program package. The MO calculation of [**4**]-$PF_6 \cdot H_2O$ shows that the Mo$-\mu_3$-S bonding orbital expands in the directions of Hb2, He2, and Hh2, which may cause the upfield shift of these proton signals (see Supporting Information Figure 2).[27] The calculated (μ_3-S)$\cdots$H distances are as follows: μ_3-S$-$Hh2 = 2.66 Å, μ_3-S$-$He2 = 2.69 Å, and μ_3-S$-$Hb2 = 2.71 Å. We think that the shielding of the proton nucleus by the electrons becomes greater as the H$\cdots$(μ_3-S) distance becomes shorter. The remaining six signals (blue) can be divided into two groups (6.18 (1H, t), 8.10 (1H, d), 8.13 ppm (1H, d) and 6.40 (1H, t), 8.16 (1H, d), 8.25 ppm (1H, d)); however, the assignment of each set of the signals to either pyrazole ring **c** or **i** is impossible. Since coalescence of the four signals (Hf1 and Hh1; Hf3 and Hh3) of [**4**]$PF_6 \cdot H_2O$ occurs at higher temperatures (D and E), the pink signals are assigned to the protons attached to pyrazole ring **f**.

Conclusion

We have prepared clusters with hindered hydrotris(pyrazolyl)borate (Tp) ligands, $[Mo_3S_4Tp_3]^+$ (**3**) and $[Mo_3OS_3Tp_3]^+$ (**4**), and we have also successfully isolated $[Mo_3FeS_4ClTp_3]$ (**5**) and $[Mo_3FeS_4BrTp_3]$ (**6**) clusters from the reaction of **3** with metallic iron. It became clear that complex **3** functions as a metal-complex ligand for preparing a novel mixed-metal complex even in nonaqueous solvents.

Supporting Information Available: Drawings of the atomic orbital components of the HOMOs, $[Mo_3S_4Tp_3]^+$ (Figure 1) and $[Mo_3OS_3Tp_3]^+$ (Figure 2), and X-ray crystallographic data in CIF format. This material is available free of charge via the Internet at http://pubs.acs.org.

IC060293I

(26) Geiger, W. E.; Ohrenberg, N. C.; Yeomans, B.; Connelly, N. G.; Emslie, D. J. H. *J. Am. Chem. Soc.* **2003**, *125*, 8680.

(27) Details of the MO calculations are currently under investigation and will be reported elsewhere.